E-ISSN-2580-7129
Print- ISSN-1978-6107

TECHNO: JURNAL PENELITIAN
Journal homepage: http://ejournal.unkhair.ac.id/index.php/Techno
Volume 14 Number 01 May 2025 DOI: https://doi.org/10.33387/tjp.v14i1.9726

Identification of Eruption Centers, Volcanic Products, Vegetation Stress, and Lineament Structures in the Mount Raung Geothermal Prospect Area Using Landsat-8 and Sentinel-1A Data Processing

Nanda Hanyfa Maulida

Department of Geophysical Engineering, Universitas Lampung, Indonesia, nandahanyfa@eng.unila.ac.id

Received : 18-04-2025
Accepted : 13-05-2025
Available online : 30-05-2025

ABSTRACT

Mount Raung is one of the active volcanic mountains which have geothermal potential. To investigates the Mount Raung geothermal prospect area in East Java, Indonesia, we use remote sensing method with Landsat-8 and Sentinel-1A data. The analysis focuses on identifying eruption centers, mapping volcanic products, assessing vegetation stress, and delineating lineament structures to provide an initial overview of the prospect zone in the area. Remote sensing methods were applied through image processing techniques including NDVI analysis, optical band composites, and radar-based structural mapping. The results indicate that Mount Raung has a large, dry caldera with multiple eruption centers and significant volcanic deposits. Several areas showed vegetation stress, potentially linked to surface geothermal manifestations. Structural analysis using SAR data revealed high lineament density, especially in the southwestern and southern regions of Mount Raung, which also coincide with vegetation stress zones. These areas are considered to have high geothermal potential due to favorable permeability conditions. The integration of optical and radar data expected to be an effective approach in the preliminary exploration of geothermal resources.

Keywords: Remote sensing, NDVI, Geothermal exploration, Structural lineaments, Mount Raung

ABSTRAK

Gunung Raung merupakan salah satu gunung berapi aktif yang memiliki potensi geotermal. Untuk menyelidiki prospek geotermal di wilayah Gunung Raung, Jawa Timur, Indonesia, digunakan metode penginderaan jauh dengan data Landsat-8 dan Sentinel-1A. Analisis difokuskan pada identifikasi pusat erupsi, pemetaan produk vulkanik, penilaian *vegetation stress*, serta delineasi struktur kelurusan (*lineament*) guna memberikan gambaran awal zona prospek geotermal di wilayah tersebut. Metode penginderaan jauh diterapkan melalui teknik pengolahan citra, termasuk analisis NDVI, komposit pita optik (*optical band composites*), dan pemetaan struktur berbasis radar. Hasil analisis menunjukkan bahwa Gunung Raung memiliki kaldera yang luas dan kering dengan beberapa pusat erupsi serta endapan vulkanik yang signifikan. Beberapa wilayah menunjukkan indikasi stres pada vegetasi, yang kemungkinan berkaitan dengan manifestasi geotermal di permukaan. Analisis struktur menggunakan data SAR mengungkapkan kepadatan kelurusan yang tinggi, khususnya di wilayah barat daya dan selatan Gunung Raung, yang juga bertepatan dengan zona stres vegetasi. Wilayah-wilayah ini dianggap memiliki potensi geotermal tinggi karena kondisi permeabilitas yang mendukung. Integrasi data optik dan radar ini diharapkan menjadi pendekatan yang efektif dalam eksplorasi awal sumber daya geotermal.

Kata kunci: *Remote sensing*, NDVI, Eksplorasi geotermal, Struktur kelurusan, Gunung Raung

INTRODUCTION

Remote sensing is a method used to obtain information about an object or area through electromagnetic radiation without making direct contact with the observed object or region (Hoerig & Kuehn, 2000; Pisharoty, 1983). According to the American Society for Photogrammetry and Remote Sensing (ASPRS), remote sensing is defined as the art, science, and technology of obtaining reliable information about physical objects and the environment through the process of recording, measuring, and interpreting imagery and digital representations of energy patterns acquired by non-contact sensor systems (Singh et al., 2020).

Based on the energy source detected by satellites, remote sensing is classified into two types: passive and active. Passive remote sensing utilizes natural energy, such as reflected sunlight or emitted thermal/ microwave radiation, and captures this reflection or emission from objects. Active remote sensing generates its own energy, transmits it toward the Earth, and receives the reflected signal from observed objects (Patel et al., 2014; Pellikka & Rees, 2009; Rott, 2000). The principles of active and passive remote sensing can be seen in Figure 1. Source 1 (e.g., the sun) emits radiation that is reflected by the Earth's surface and detected by sensors, representing passive remote sensing; whereas Source 3 emits its own energy (such as radar) and detects the backscattered signal, representing active remote sensing. Source 2 represents emitted radiation from the Earth's surface (e.g., thermal energy), which can also be captured by sensors for environmental analysis. Based on the wavelength detected by the sensor, remote sensing is divided into visible-shortwave infrared (optical), thermal infrared (TIR), and synthetic aperture radar (SAR)

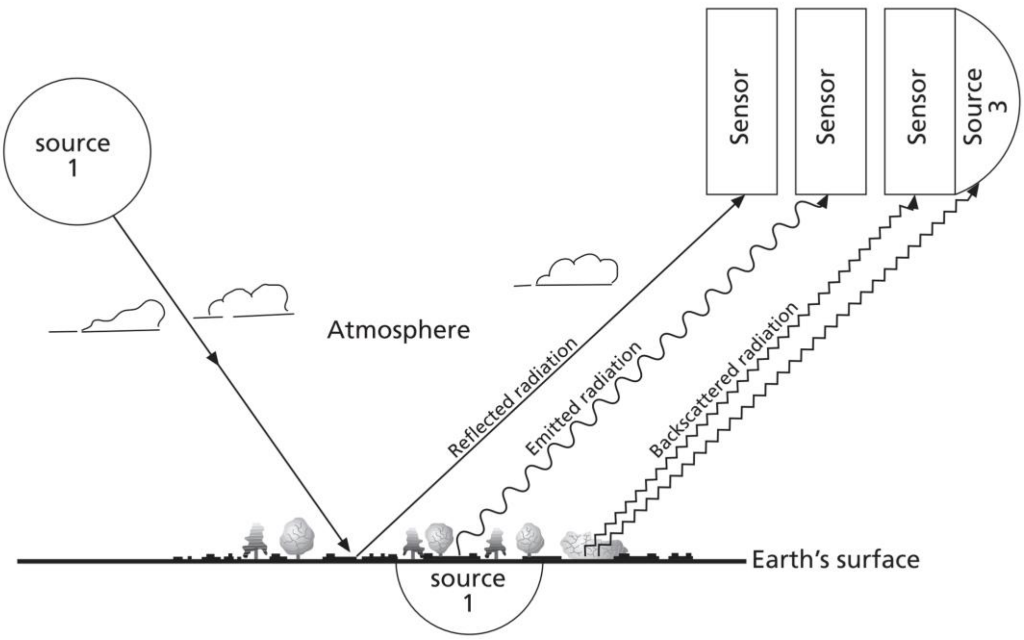

Figure 1. The principle of the energy source and receiving sensor in remote sensing
(Image source: Jong et al, (2004)

Remote sensing has been widely used across various scientific disciplines related to the Earth's surface. In geothermal exploration, remote sensing is one of the commonly used methods during the preliminary exploration stage before conducting direct field surveys. Remote sensing is highly useful in the early stages of geothermal exploration because it can efficiently identify surface thermal anomalies and active fault zones while covering large areas (Pasqua & Verdoya, 2014). Information about the surface conditions of the target exploration area can be more easily monitored using satellite imagery, whether optical or radar data. Satellite image analysis, such as Landsat, ASTER, and SAR, helps detect geological structures like fractures and high-permeability zones, which could potentially serve as pathways for geothermal fluid flow (Pasqua & Verdoya, 2014).

In preliminary exploration, aerial photo interpretation and satellite imagery are used to identify the types and distribution of rocks, geological structures, and landforms through tonal variations and lineations that can be recognized in the aerial photos or satellite images (Bhan & Krishnanunni, 1983; van der Meer et al., 2014). Investigation methods have continued to evolve, one of which is the NDVI (Normalized Difference Vegetation Index) investigation, used to detect the presence of stressed vegetation, which can be an indicator of surface heat manifestations (Gemitzi et al., 2021; Saepuloh et al., 2024; Syawalina et al., 2022). Structural identification can be used to localize areas with good permeability (Arrofi et al., 2022; Putri & Daud, 2023). The locations of eruption centers can serve as indicators of heat sources in a geothermal system. By integrating this data, exploration activities will be more focused and well-managed.

This study was conducted at Mount Raung in East Java (Figure 2), with the primary objective of performing a preliminary geothermal exploration survey by mapping structural features, morphology, and vegetation stress. The location lies within the Ijen-Raung mountain range, a region that is geologically recognized for its geothermal potential, further supporting its suitability as a target for exploration. Therefore, a remote sensing-based preliminary study is highly relevant for identifying surface indicators and prospective zones, that can be followed up with field surveys and more detailed geophysical methods.

Figure 2. Mount Raung location

METHODOLOGY

The data used in this study consist of optical and SAR (Synthetic Aperture Radar) imagery. The optical imagery is obtained from Landsat-8 OLI (Operational Land Imager), selected based on scenes with the lowest cloud cover to ensure optimal surface visibility. The radar imagery is acquired from Sentinel-1A IW Level-1 GRD products, using VV+VH polarization for the descending mode and VV polarization for the ascending mode. Data were collected using the USGS Earth Explorer and Copernicus Open Access Hub platforms. Analytical techniques include NDVI (Normalized Difference Vegetation Index) calculation for assessing vegetation stress (Asokawaty et al., 2017; Kusumadewi & Suryantini, 2024), optical band composite analysis for morphology, erruption center and erruption product identification (Saepuloh et al., 2004), and lineament extraction from SAR data (Choudhury et al., 2025) potentially related to geothermal activity.

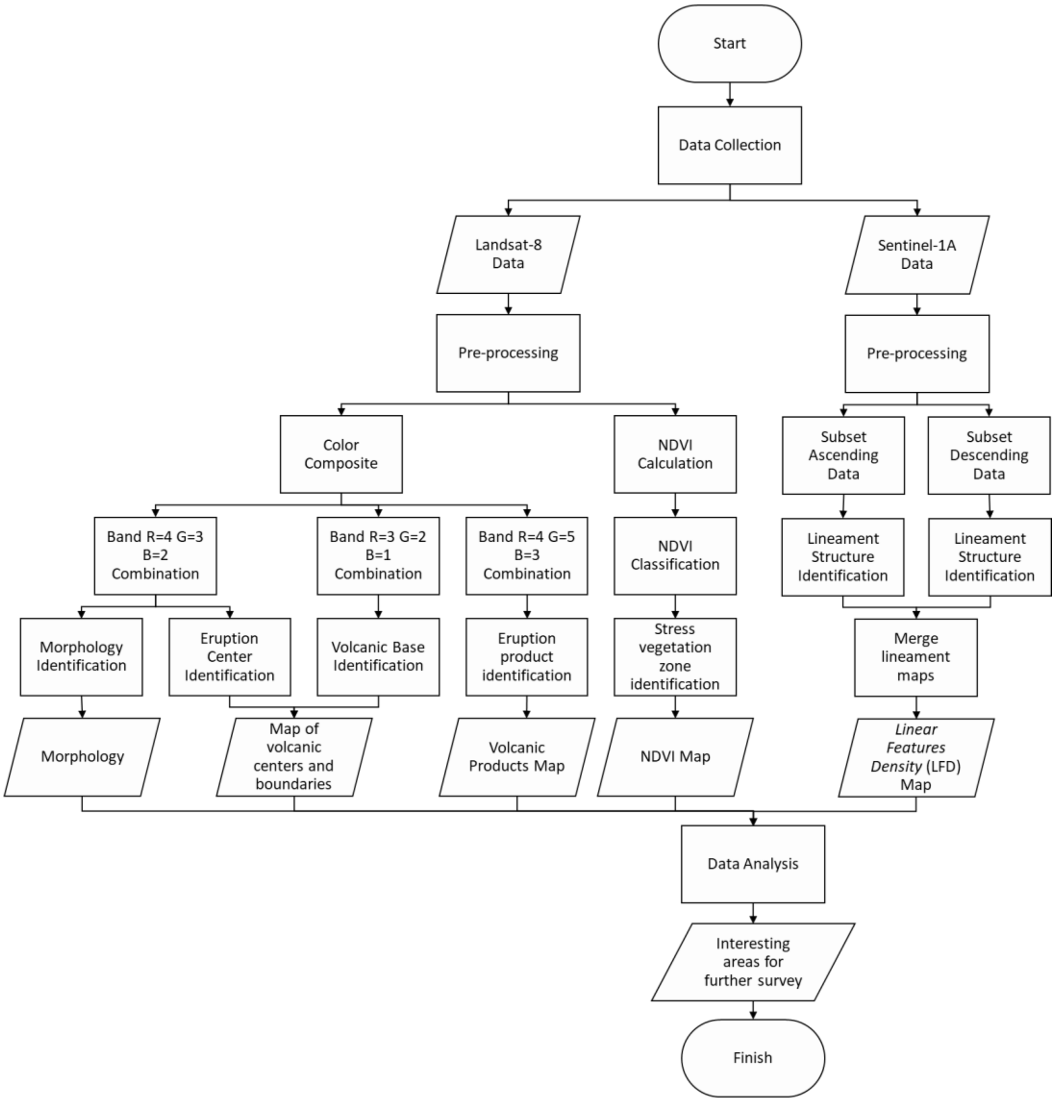

Figure 3. Research flowchart

In data processing, several software tools were used, such as ENVI 5.1, ILWIS 3.3, SNAP, and ArcMap 10. The data processing steps are shown in Figure 3. The initial stage involved preprocessing Landsat-8 imagery, which included radiometric and atmospheric correction to enhance data quality, as well as data subseting to focus on the study area. Subsequently, preprocessing of Sentinel-1A data was carried out, including radiometric calibration, terrain correction, data subseting, and speckle filtering to reduce noise in the radar images.

The next step involves identifying the morphology, base of the volcano, and eruption centers using a natural color composite to observe surface features, followed by several color composites to locate eruption centers and define the base boundary. Volcanic products are then identified using a false color composite based on their spectral characteristics. Thermal anomalies are detected using the Normalized Difference Vegetation Index (NDVI), classifying areas into high, moderate, and low vegetation zones, with stressed vegetation indicating potential anomalies. Sentinel-1A data from both ascending and descending orbits are analyzed to identify circular features and lineaments, and the results are combined to create a lineament density map for inferring subsurface structures. Finally, all data are integrated for a comprehensive geological and volcanological interpretation of the area.

RESULTS AND DISCUSSION

The Morphology of Mount Raung

Mount Raung is one of the volcanoes located in the Ijen Mountain complex, East Java. Based on optical imagery processing, a natural color composite with a combination of bands 4-3-2 was created to observe the actual condition of Mount Raung (Figure 4). From the image, it can be seen that Mount Raung has a conical shape with a large and dry caldera as its main eruption center. A dome or mound formation is also visible at the center of the caldera, indicating a positive morphology of Mount Raung. Apart from the dry caldera, Mount Raung is surrounded by dense vegetation.

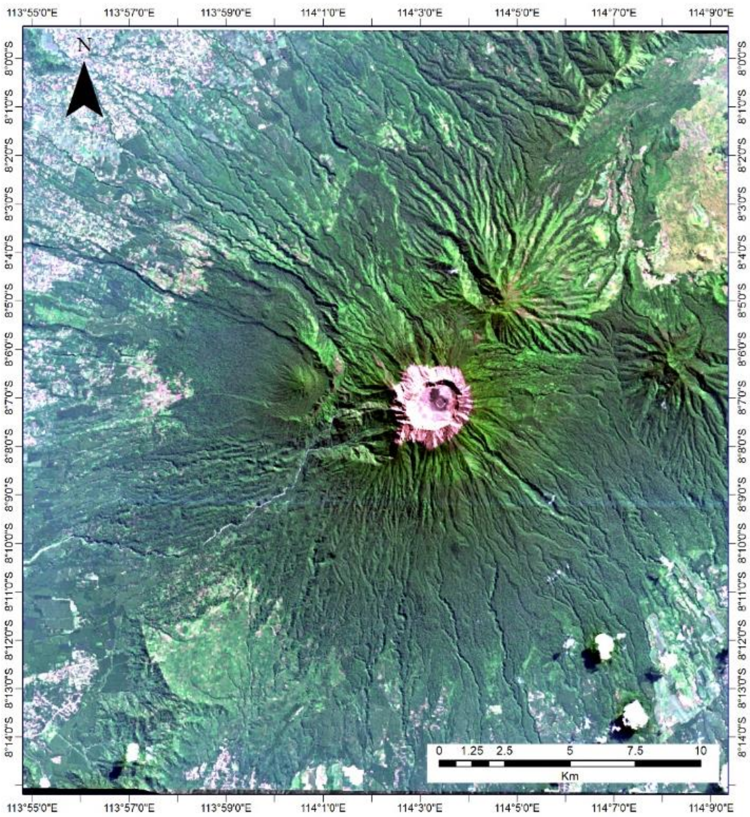

Figure 4. True colour composite of Mount Raung

Using different color composites, additional eruption centers around Mount Raung were identified. The composite used was a band combination of 3-2-1, as shown in Figure 5. From the observation of this color composition, five eruption centers are detected, with the eruption center to the west identified as a mound (or "gumuk") of Mount Raung. The base of Mount Raung was also identified from the same imagery.

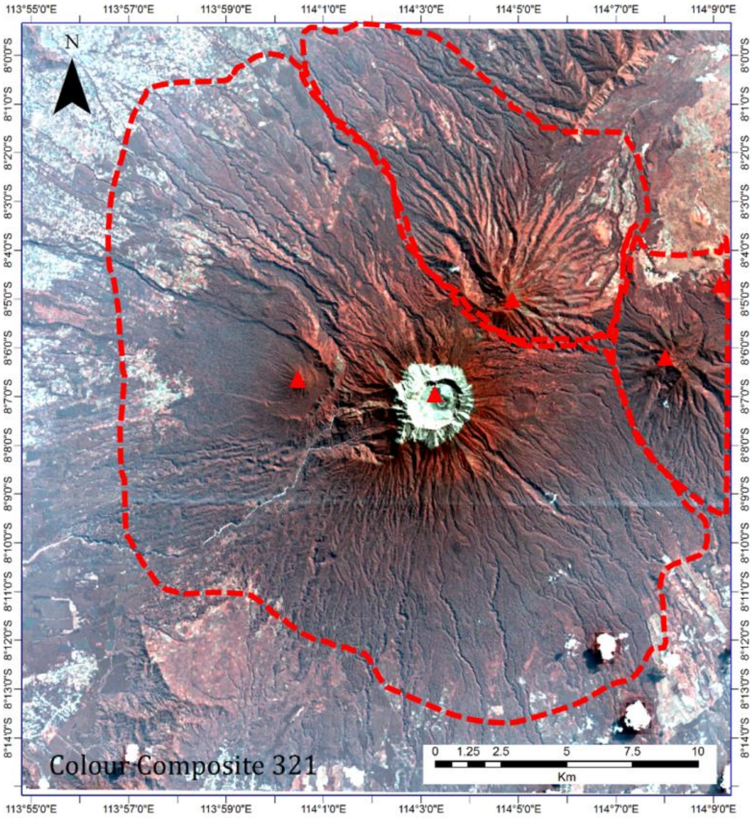

Figure 5. Eruptions center (red triangle) and base (red dash line) of Mount Raung

Volcanic Product of Mount Raung

To identify the volcanic products of Mount Raung, several color composites were tested using different band combinations. After several trials, the band combination of 4-5-3 was chosen to identify volcanic products. The identification was based on differences in color, contrast, brightness, and texture in the imagery. The classification of volcanic products can be seen in Figure 6. The red line indicates products likely resulting from Mount Raung's eruptions, while other colors represent products from surrounding volcanoes.

Vegetation Distribution and Detection of Vegetation Stress

The Normalized Difference Vegetation Index (NDVI) indicates the 'greenness' level of vegetation. In geothermal studies, NDVI is used to detect areas experiencing vegetation stress, which may result from surface thermal manifestations. The NDVI results are shown in Figure 7, with values ranging from -0.1 to 0.99. These results were compared with the natural color composite to classify vegetation conditions.

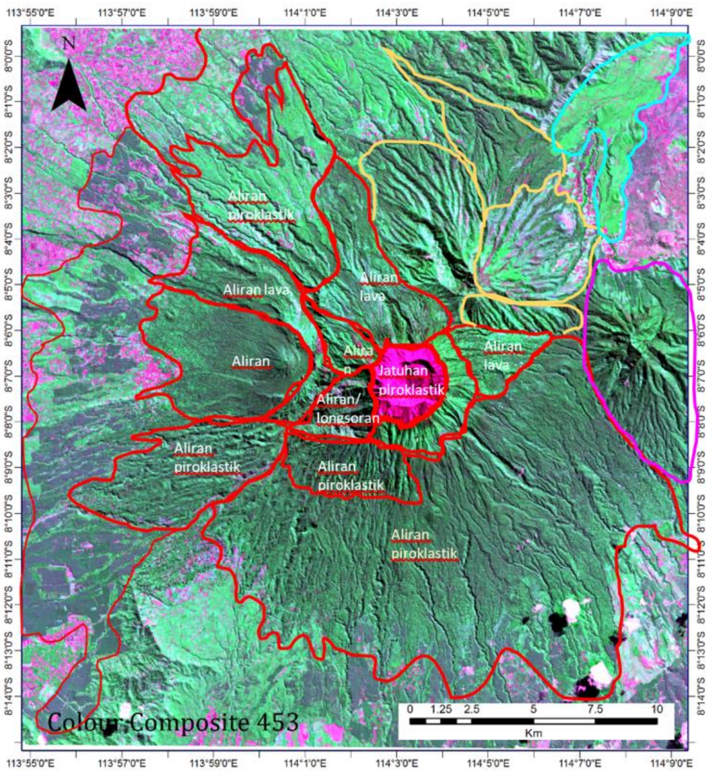

Figure 6. Classification of Mount Raung eruption products

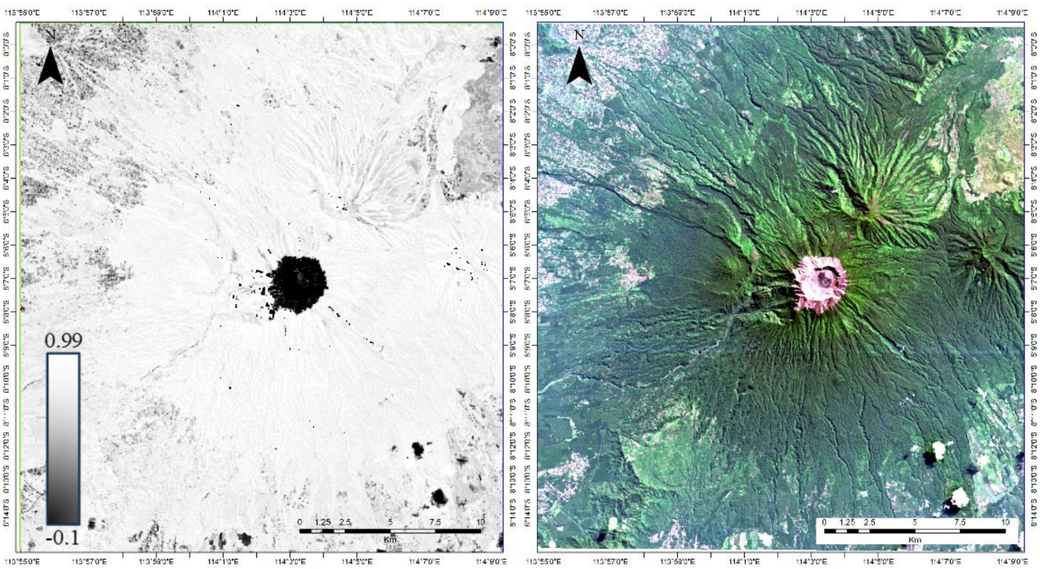

Figure 7. The NDVI calculation image (left) is compared with the natural color composite (right)

Healthy vegetation absorbs most of the red wavelengths of sunlight and reflects higher near-infrared wavelengths, resulting in a high NDVI value. In contrast, dead or stressed vegetation (less healthy) reflects more red wavelengths and fewer near-infrared wavelengths, leading to a lower NDVI value. Based on the comparison, the NDVI classification yielded low values of less than 0.25, moderate values ranging from 0.25 to 0.80, and high values greater than 0.80 (Figure

8). By cross-referencing the NDVI classification map with the natural color composite, it is hypothesized that areas with low NDVI values correspond to stressed vegetation locations.

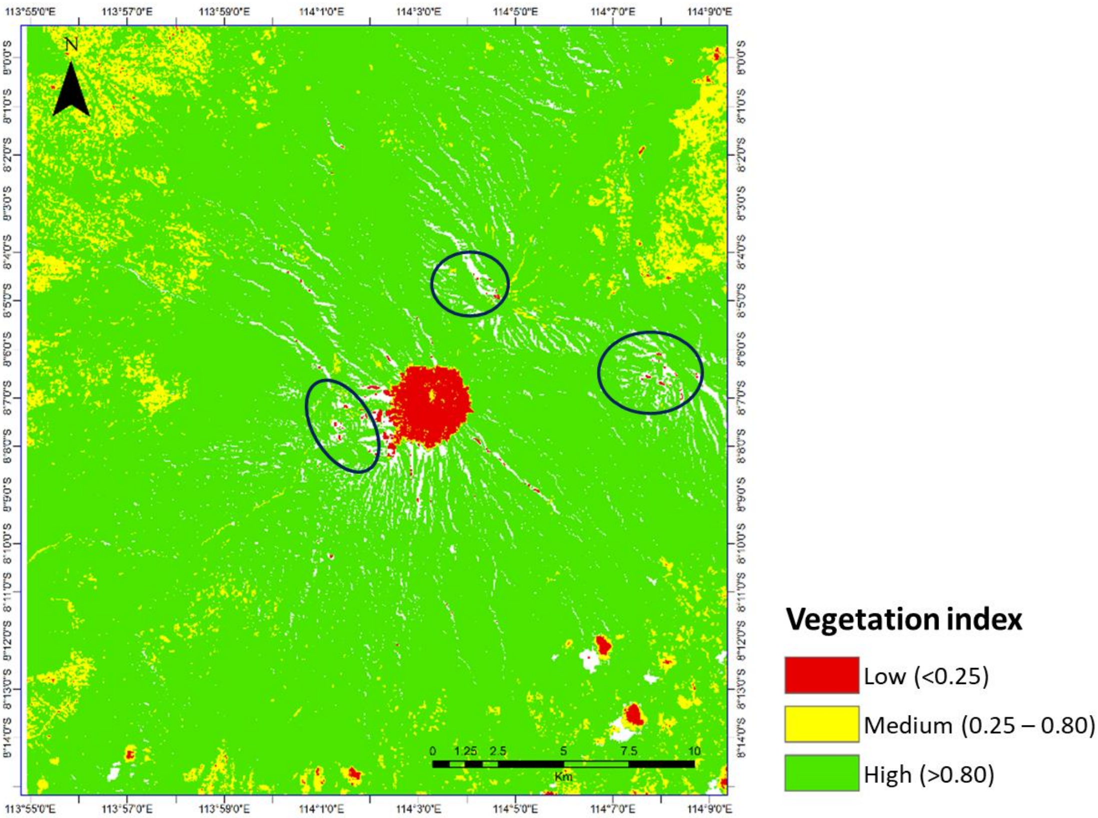

Figure 8. NDVI Classification and locations suspected of experiencing vegetation stress (black circles)

Identification of Circular Features and Structures with SAR Imagery

Besides being used for identifying natural features, morphology, and vegetation distribution, optical imagery can also be used to identify structures in an area. However, because most geothermal fields are covered by dense vegetation, structural identification tends to be more challenging. Therefore, another type of satellite imagery, namely radar/SAR, is used, as it employs longer wavelengths capable of detecting structures that are obscured by the vegetation canopy.

The radar imagery used is from Sentinel-1A with a C-band sensor. There are two data acquisition modes based on the sensor's movement relative to the object: ascending and descending. Ascending data is acquired when the satellite moves northward with the sensor pointing east, while descending data is collected when the satellite moves southward with the sensor facing west (Figure 9).

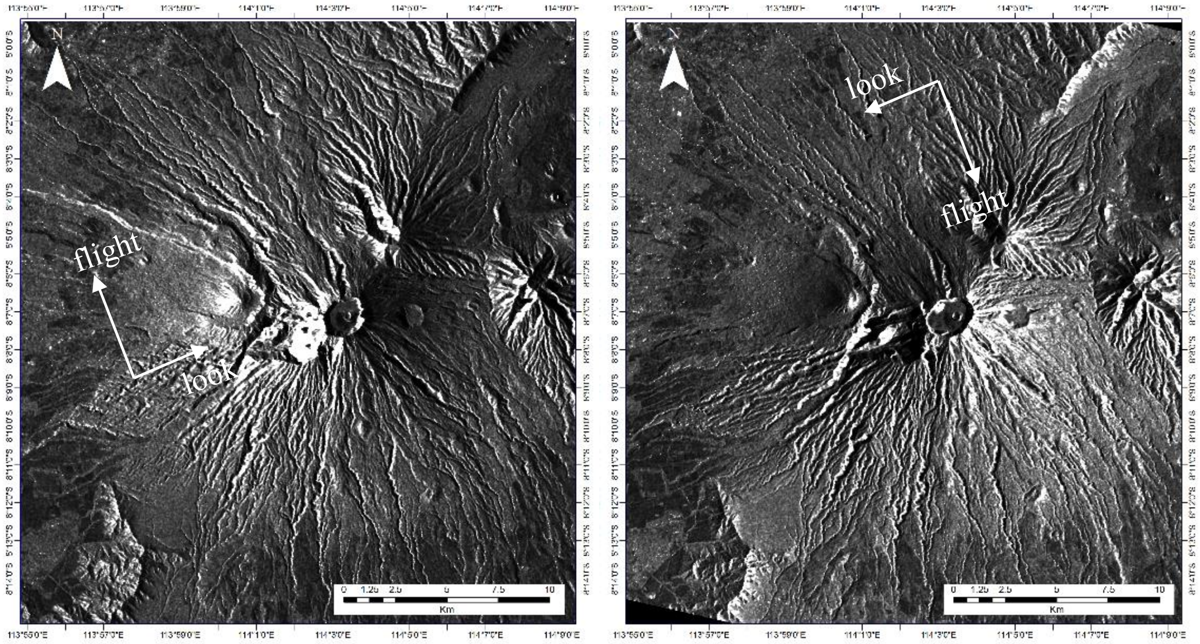

Figure 9. Sentinel-1A imagery with data acquisition in ascending (left) and descending (right) modes

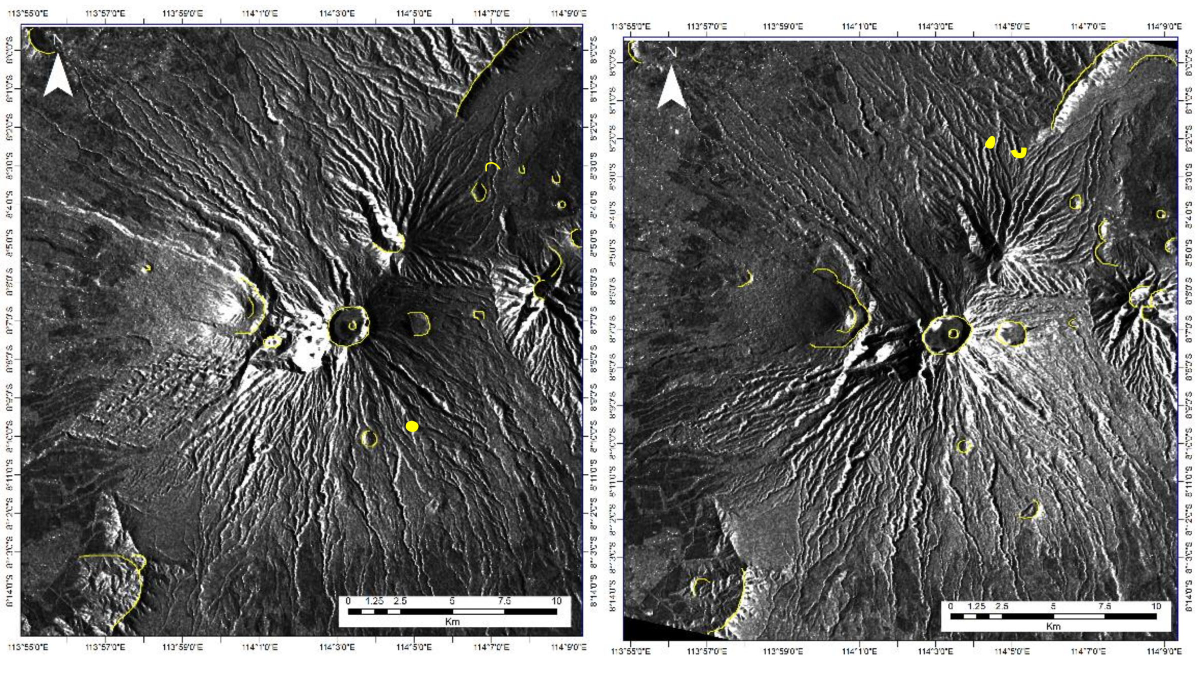

Figure 10. Identification of circular features (yellow lines) from ascending data (left) and descending data (right)

The first identified structure is the circular feature, which is characteristic of volcanic eruption centers. As shown in Figure 10, circular structures are easily identifiable and are more clearly visible compared to those observed using optical data. The number of these structures is also greater than in the optical data observations, although this requires validation through direct field observations. Some structures that are less distinct in the ascending data are more clearly visible in the descending data, and vice versa.

Next, the identification of lineaments from both datasets was carried out. By combining the two images with different data acquisition directions, we can generate structures more clearly. Similar to the identification of circular features, structures that are not visible in the ascending data can be observed in the descending data, and vice versa (Figure 11).

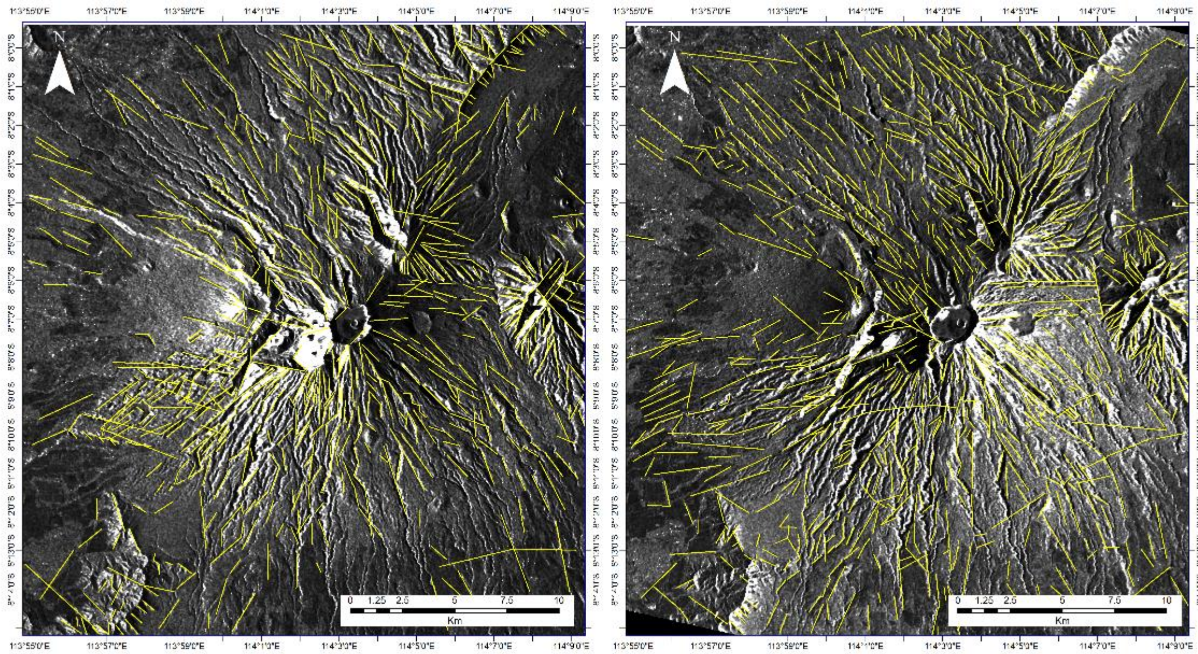

Figure 11. Identification of lineaments from ascending data (left) and descending data (right).

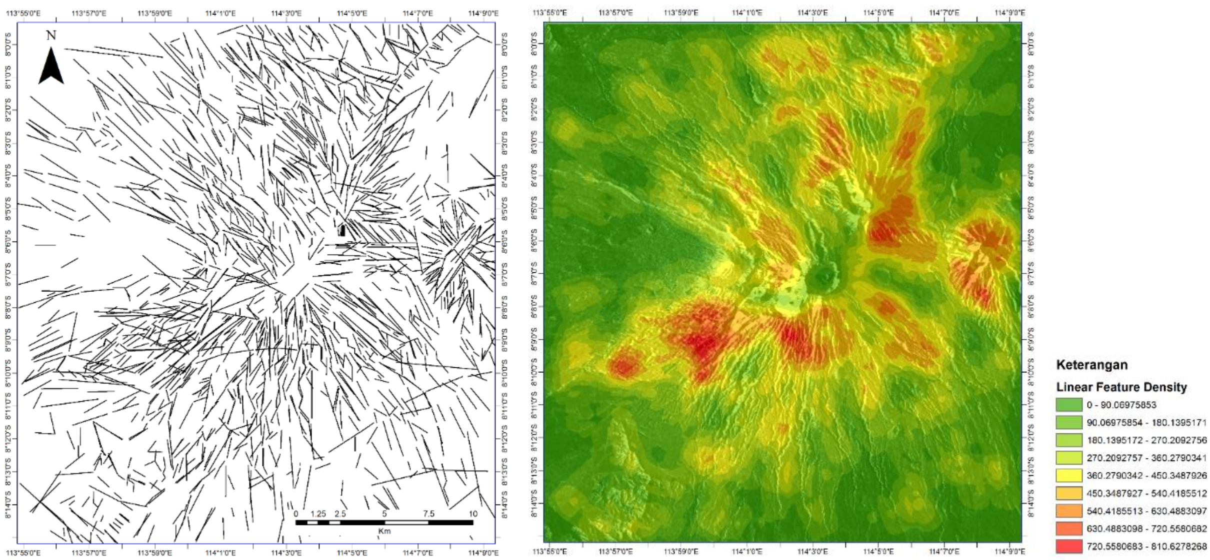

Figure 12. Identified lineaments from ascending and descending data (left) and distribution of lineament density per unit area of Mount Raung (right)

The results of the lineament identification from the two datasets were then combined and used for structural analysis using the Linear Features Density (LFD) method. The total lineaments from both ascending and descending data are shown in Figure 12 (left), and the LFD map is presented in Figure 12 (right). High lineament density is marked in red and is distributed across several zones around Mount Raung. The highest intensity is found in the Southwest and South of Mount Raung. High intensity is also observed at the boundary between Mount Raung and other volcanoes to the east. If the lineaments in these areas are the result of fault or fracture structures, it can be assumed that these locations represent prospective zones with good rock permeability.

CONCLUSION

The results of the image data processing, both optical and radar, are highly useful as considerations for conducting field exploration. Optical data shows Mount Raung as a stratovolcano characterized by a dry crater and several eruption centers. The volcanic products from Mount Raung include lava flows, pyroclastic flows, and pyroclastic fall deposits. Based on NDVI analysis, several locations around the volcano are suspected to be experiencing vegetation stress, indicated by NDVI values less than 2.5. In terms of structural features, a total of 22 circular features were identified from the ascending data, and 23 from the descending data. The highest lineament intensity is observed in the Southwest and South of Mount Raung, as well as along the boundary between Mount Raung and neighboring volcanoes to the east. These findings suggest that the Southwest region of Mount Raung, with its vegetation stress and high lineament density, is an area of interest for further field surveys.

Based on the findings, it is suggested that future research should focus on conducting detailed field surveys in the Southwest region of Mount Raung. This area shows strong indications of vegetation stress and high lineament density, which may point to potential geothermal activity or fault zones with good rock permeability. A comprehensive field investigation, including geological mapping and geophysical surveys, could provide valuable insights into the subsurface structure and geothermal potential of this region.

ACKNOWLEDGEMENTS

The author would like to thank all parties who have provided support and contributions in the implementation of this research. Special thanks are extended to the data collection team at Mount Raung.

REFERENCES

Arrofi, D., Abu-Mahfouz, I. S., & Prayudi, S. D. (2022). Investigating high permeable zones in non-volcanic geothermal systems using lineament analysis and fault fracture density (FFD): Northern Konawe Regency, Indonesia. *Geothermal Energy*, *10*(1), 29. https://doi.org/10.1186/s40517-022-00241-3.

Asokawaty, R., Nugroho, I., Satriana, J., Hafidz, M., & Suryantini. (2017). Preliminary study of Songa-Wayaua geothermal prospect area using volcanostratigraphy and remote sensing analysis. *IOP Conference Series: Earth and Environmental Science*, *103*(1), 012020. https://doi.org/10.1088/1755-1315/103/1/012020.

Bhan, S. K., & Krishnanunni, K. (1983). Applications of remote sensing techniques to geology. In *Proceedings of the Indian Academy of Sciences Section C: Engineering Sciences*, *6*, 297–311. https://doi.org/10.1007/BF02881136.

Choudhury, N., Mitra, A. K., Nath, B., & Lindsay, M. D. (2025). Lineament extraction and structural mapping using Landsat-9 OLI and Sentinel-1 SAR data in the Proterozoic North Singhbhum Mobile Belt, Eastern India. *Geosystems and Geoenvironment*, *4*(3), 100392. https://doi.org/10.1016/j.geogeo.2025.100392.

Gemitzi, A., Dalampakis, P., & Falalakis, G. (2021). Detecting geothermal anomalies using Landsat 8 thermal infrared remotely sensed data. *International Journal of Applied Earth Observation and Geoinformation*, *96*, 102283.

Hoerig, B., & Kuehn, F. (2000). Remote sensing: an overview of physical fundamentals. In F. Kuehn, T. V. V. King, B. Hoerig, & D. C. Peters (Eds.), *Remote Sensing for Site Characterization* (pp. 5–8). Springer. https://doi.org/10.1007/978-3-642-56978-4_2.

Jong, S. M. D., Meer, F. D. V. D., & Clevers, J. G. P. W. (2004). Basics of remote sensing. In S. M. D. Jong & F. D. V. D. Meer (Eds.), *Remote Sensing Image Analysis: Including The Spatial Domain* (Vol. 5, pp. 1–15). Springer Netherlands. https://doi.org/10.1007/978-1-4020-2560-0_1.

Kusumadewi, I., & Suryantini, S. (2024). Monitoring of thermal variations in geothermal activity in the Mount Sirung Field, East Nusa Tenggara with satellite imageries. In *ITB Graduate School Conference*, *4*(1), Article 1. https://gcs.itb.ac.id/proceeding-igsc/igsc/article/view/296.

Pasqua, C., & Verdoya, M. (2014). Remote Sensing Techniques as a Tool for Geothermal Exploration: The Case Study of Blawan Ijen, East Java. In *EGU General Assembly Conference Abstracts*, 5942. https://ui.adsabs.harvard.edu/abs/2014EGUGA..16.5942P/abstract.

Patel, U., Patel, R., & Patel, N. (2014). Study about remote sensing, its process, types, applications and advantages. *International Journal of Engineering Sciences & Research Technology*, *3*(12), 267–269.

Pellikka, P., & Rees, W. G. (Eds.). (2009). Principles of remote sensing. In *Remote Sensing of Glaciers*. CRC Press.

Pisharoty, P. R. (1983). Introduction to remote sensing. In *Proceedings of the Indian Academy of Sciences Section C: Engineering Sciences*, *6*(2), 97–107. https://doi.org/10.1007/BF02842927.

Putri, F. F., & Daud, Y. (2023). Identification of permeable zone in Kepahiang geothermal prospect area (Bengkulu) using integration of fault and fracture density method with gravity data. In *AIP Conference Proceedings*, *2798*(1). https://pubs.aip.org/aip/acp/article-abstract/2798/1/020052/2904168.

Rott, H. (2000). Physical principles and technical aspects of remote sensing. In G. A. Schultz & E. T. Engman (Eds.), *Remote Sensing in Hydrology and Water Management* (pp. 15–39). Springer. https://doi.org/10.1007/978-3-642-59583-7_2.

Saepuloh, A., Sumintadireja, P., & Suryantini. (2004). Geologi Gunung Guntur, Kabupaten Garut, berdasarkan interpretasi citra ASTER. *Buletin Geologi*, *36*(3), 91–105. https://doi.org/10.33332/jgsm.geologi.v18i4.338.

Saepuloh, A., Yoni, D. R., Akrom, F. M., Shrestha, D. P., & Van der Meer, F. (2024). Thermal and vegetation indices of geothermal steam spots derived by high resolution images and field verifications. *Geothermics*, *123*, 103101. https://doi.org/10.1016/j.geothermics.2024.103101.

Singh, V., Pathak, D., Sayyeda, S., & Sheera, A. (2020). *Importance and Applications of Remote Sensing in Agriculture*. https://consensus.app/papers/importance-and-applications-of-remote-sensing-in-singh-pathak/172ebc9cb20c52deb21d27feb5a55b63/

Syawalina, R. K., Ratihmanjari, F., & Saputra, R. A. (2022). Identification of the relationship between LST and ndvi on geothermal manifestations in A preliminary study of geothermal exploration using landsat 8 OLI/TIRS imagery data capabilities: Case study of toro, central sulawesi. In *PROCEEDINGS, 47th Workshop on Geothermal Reservoir Engineering*. https://pangea.stanford.edu/ERE/db/GeoConf/papers/SGW/2022/Syawalina.pdf

Van der Meer, F., Hecker, C., van Ruitenbeek, F., van der Werff, H., de Wijkerslooth, C., & Wechsler, C. (2014). Geologic remote sensing for geothermal exploration: A review. *International Journal of Applied Earth Observation and Geoinformation*, *33*, 255–269. https://doi.org/10.1016/j.jag.2014.05.007.